JAUES

Journal of Al-Azhar University Engineering Sector

Vol.15, No. 56, July, 2020, 763-775

NUMERICAL ANALYSIS OF TRANSPORT PHENOMENA IN A STIRLING REGENERATOR

M. Ameen*, W.Aboelsoud, A. E. Hussin, and M. M. Kamal
Department of Mechanical power engineering, AinShams University,Cairo, Egypt
*Corresponding Author E-mail: mohamed.ameen710@gmail.com

ABSTRACT
In the context of increasing the efficiency of alternative energy sources applications, Stirling engines attracted researchers to study the engine performance since it is an external heat addition engine that can work with renewable heat resources or with waste heat from plants working with fossil fuels with an efficiency equivalent to Carnot efficiency. Additional advantages exist, such as quiet operation and lower emissions than internal combustion engines. The regenerator is an essential part of Stirling engine as it plays a vital role in its operation especially in the two isochoric heat transfer processes representing a heat barrier and transferring heat to the fluid in the first half of the cycle and transferring heat from the fluid in the second half of the cycle. In the last two decades, the development of CFD methods made it possible to study transport phenomena without the need for costly experimental methods and can give more detailed information about the effects of geometrical parameters than the theoretical or analytical methods. The purpose of this study is to develop a model for an alpha type Stirling engine and using the advantage of geometrical representation in CFD models to study the effect of changing regenerator geometry on engine performance. Validation of the model against results in the literature was performed. Results showed that the dimensionless work parameter was 0.011 for the novel geometry while it was 0.065 for the original regenerator, decreasing the engine speed increased the dimensionless work parameter to 0.018, effects of changing apex angle and wall thickness on the dimensionless parameter were investigated.

KEYWORDS: Stirling Engine, Stirling Engine Regenerator, CFD, Porous media, and Oscillating flow.

التحليل العددي لظواهر الانتقال داخل مسترجع حراري

محمد أمين*، وليد أبو السعود*، أحمد حسين، ومحمود كمال
قسم هندسة القوى الميكانيكية، جامعة عين شمس،القاهرة ، مصر
*البريد الاليكتروني للباحث الرئيسي: E-mail : mohamed.ameen710@gmail.com

الملخص
في سياق زيادة كفاءة تطبيقات مصادر الطاقة البديلة, جذبت محركات ستيرلنج الباحثين لدراسة آداؤه و ذلك لكونه محرك احتراق خارجي يمكنه العمل مع مصادر حرارة قابلة للتجدد أو مصادر حرارة يتم إهدارها في المصانع التي تستخدم الوقود الحفري و بكفاءة تعادل كفاءة محرك كارنو بالإضافة لمميزات أخرى مثل: التشغيل الهادئ و إنبعاثات أقل من محركات الاحتراق الداخلي. يعد المسترجع جزءا مهما من محرك ستيرلنج و ذلك لدوره الحيوي في تشغيله ، خاصة في عمليتي نقل الحرارة التي تتم في حيز ثابت حيث يمثل حاجزا حراريا ينقل الحرارة إلى المائع في النصف الأول من الدورة و يأخذ حرارة من المائع في النصف الثاني من الدورة. في العقدين الأخيرين تطورت طرق ديناميكا الموائع الحسابية بشكل ملحوظ

حيث أصبحت دراسة ظواهر الانتقال ممكنة و بدون الحاجة لطرق تجريبية مكلفة بالإضافة إلى ميزة إعطاء معلومات إضافية عن تأثير الأشكال الهندسية على الأداء أكثر من الطرق التحليلية و النظرية. الهدف من هذه الدراسة هو تطوير نموذج محاكاة لمحرك ستيرلنج و الاستفادة من ديناميكا الموائع الحسابية في معرفة تأثير تغيير شكل المسترجع الحراري على أداء المحرك. تم إختبار التحقق من صحة نتائج النموذج بمقارنة النتائج مع نتائج دراسات سابقة. أظهرت النتائج أن معامل الشغل الذي ليس له بعد كان 0.011 للشكل الهندسي الجديد للمسترجع بينما كان 0.065 للشكل الأصلي للمسترجع ، كما أظهرت أيضا أن تقليل سرعة المحرك يزيد من هذا المعامل إلى 0.018 ، كما تم دراسة تأثير تغيير زاوية المسترجع و سمك المسترجع على المعامل.

الكلمات المفتاحية: محرك ستيرلنج ،مسترجع محرك ستيرلنج ، ديناميكا الموائع الحسابية ، الوسائط المسامية ، والسريان الترددي.

Nomenclature

a0	half piston stroke [m]	Th	temperature of heater walls [K]
Cf	friction coefficient	u	velocity of fluid [m/s]
Cp	heat capacity of the gas at constant pressure [J/Kg K]	Vclc	clearance volume at cold cylinder [m3]
dh	hydraulic diameter [m]	Vcle	clearance volume at hot cylinder [m3]
dw	wire diameter [m]	Vcooler	volume of cooler [m3]
dz	thickness [m]	Vheater	volume of heater [m3]
F	volume force source term	Vregenerator	volume of regenerator [m3]
k	permeability	Vsc	swept volume at cold cylinder [m3]
K	thermal conductivity of the gas [W/m K]	Vse	swept volume at hot cylinder [m3]
Keff	effective thermal conductivity [W/m K]	$W_{dimensionless}$	Dimensionless work
m	Mass of working fluid [Kg]	W	Work of one cycle [J]
N	speed of rotation [r.p.m]	Xp1	cold side piston displacement [m]
P	instanteneous gas pressure [Pa]	Xp2	hot side piston displacement [m]
Pcharge	charge pressure [Pa]		
Q	heat source	**Greek symbols**	
Q_{br}	mass source term	α	phase shift angle [rad]
Qoop	out of plane heat transfer	Θ	crank angle [rad]
Qp	work done by pressure changes	Ɛp	porosity
Qvd	viscous dissipation	P	density
Rs	gas constant [J/Kg K]	M	fluid dynamic viscosity [Pa.s]
t	time [s]	β_F	forcheimer coefficient
T	temperature [K]	I	the identity matrix
Tc	temperature of cooler walls [K]	Θp	Volume fraction
Tcharge	charge Temperature [K]		
Tcomp	Temperature of compression space [K]		
Te	temperature of expansion space [K]		

1. INTRODUCTION

Stirling engines are externally heated engines that can work between a heat source at a high temperature and a heat sink at a low temperature with an efficiency equivalent to the efficiency of the Carnot cycle. Thus Stirling engines can be used for applications using renewable heat energy sources or waste heat from plants using fossil fuels. The theoretical cycle for Stirling engines includes two isothermal processes at which heat is being transferred between fluid and heat source in one of them and between fluid and heat sink in the other and 2 isochoric processes at which heat is being transferred between fluid and regenerator so that at one of the two isochoric processes heat is being transferred from the fluid and at the other heat is being transferred to the fluid. The regenerator thus can be considered as a heat barrier separating the hot side from the cold side. Also, it reduces the amount of heat required to be supplied or absorbed from the fluid so that it reduces the heat input and maximizes the work output giving maximum possible efficiency. Many researchers studied the Stirling engine, and in the literature, analyses can be categorized as Zero, 1^{st}, $2^{nd,}$ and 3^{rd} order analyses. Zero-order analyses where dimensionless numbers and empirical equations are used to calculate power output and efficiency of the engine, 1^{st} order analysis (Schmidt analysis or isothermal analysis) an ideal analysis based on isothermal heat transfer and volume change following sine wave, 2^{nd} order analysis (Non-ideal adiabatic) considering compression and expansion spaces adiabatic and work output is being calculated by subtracting power losses and heat losses from ideal cycle. 3^{rd} order analysis at which spaces are divided into smaller parts using meshes and calculating variables at the nodes using equations of conservation of mass, momentum, and energy. This method is the base for all CFD approaches(Alexakis, 2013).

(Tanaka et al., 1990) studied transport phenomena of a Stirling engine regenerator in an oscillating flow experimentally for various regenerator materials (wire net, sponge metal, and sintered metal), the pressure drop, heat transfer coefficient of various materials were estimated by using friction factor, Nusselt number and Reynolds number using hydraulic diameter as representative length, a new empirical equation was found valid for the relationship between friction coefficient and Reynolds number, mean heat transfer coefficient was obtained using instantaneous temperatures during one cycle. Another empirical equation between Nusselt number and Reynolds number for wire netting was stated, a relationship between regenerator reheat loss and regenerator size was found, and a simple equation was derived that uses regenerator length, mesh diameter and mean temperatures for calculating heat transfer loss at regenerator. The effects of mesh diameter and regenerator length on the indicated thermal efficiency of the Stirling engine were investigated.

(S. C. Costa et al., 2013) derived a universal correlation in addition to two specific correlations based on 3 parameter modified Ergun equation for calculating pressure drop friction coefficient for wound woven regenerator wire matrix for Re (up to 400),porosity from 0.472 to 0.638 and diameter of 0.08 to 0.110 based on numerical finite volume analysis used at first for stacked woven wire mesh validated against experimental work of (Tanaka et al., 1990) and Gedeon et al. then expanding the analysis for the wound woven wire mesh, the wire mesh diameter significance on pressure drop computation was showed, so it was added to the 3 parameter Ergun equation. The results showed that the pressure drop friction coefficient for the wound woven wire matrix is higher than that of the stacked woven wire matrix for low Re number <100, yet it becomes the same as stacked at Re>100. The same research team (S. C. Costa et al., 2014) studied the heat transfer phenomena in porous media for both stacked and wound woven wire matrices of Stirling engine through the same ranges of Re (<400), wire diameter (0.08 to 0.11mm) and porosity (0.6 to 0.68), as in the previous work heat transfer correlations for Nusselt number were obtained from a finite volume analysis of the stacked woven wire matrices, validated against well known experimentally empirical equations which showed maximum deviation of 6% then extending the analysis to the wound woven wire matrices to obtain correlations for heat transfer for this different flow configuration, the same team studied pressure drop and heat transfer in regenerator both experimentally and numerically in (S.-C. Costa et al., 2014).

(Almajri et al., 2017) studied Stirling engine by developing a thermodynamic analytical model (using non-ideal adiabatic method) validated with experimental results then developing a CFD analysis validated with thermodynamic model and using a parametric study of the effects of various design parameters and operating conditions as regenerator porosity, charge pressure, matrix wire diameter, dead volume and hot/cold ends temperatures on the engine performance in terms of power output through predicting the P-V diagram of the engine. The parametric study was used to give recommendations for the values of porosity, wire matrix diameter temperatures of hot and cold sides, and dimensions of the heater and cooler to obtain maximum power.

(Alfarawi et al., 2016) studied the effects of dead volume and phase angle on engine performance and validated the results of the numerical model against experimental results with accuracy from 5 to 9 % in predicting indicated power the study also concluded that a phase angle of 105 degrees would give more indicated power than the 90 degrees commonly used in the literature.

(Ahmed et al., 2017) used the model developed by Al-Majri (Almajri et al., 2017) and investigated using its Stirling cycle as a Cryocooler.

(Mahkamov, 2006) studied a Biomass gamma Stirling engine using both 2nd order non-ideal adiabatic mathematical model and CFD modeling to explain the deviation of actual output power from results of 1st order model originally used in the design of the manufactured engine, based on 3D CFD with K-epsilon turbulence model for compressible flow results he suggested many design and geometry modifications to improve output power.

He also stated that the 2nd order model has a disadvantage is that it represents the engine as being one-dimensional, which makes it practically impossible to reflect the major geometrical features of the real internal gas circuit of the engine. The results from 2nd order model revealed that overall pressure loss was found to be mainly influenced by the hydraulic resistance in the regenerator this was attributed to the low porosity value of regenerator 31%; numerical study confirmed the last result and suggested that the negative effect of the hydraulic resistance increases with the speed of the engine.

One of the important conclusions of this study is that when analyzing velocity data, it is possible to detect regions in the internal gas circuit, where there are recirculation and stagnation zones and intensive vortex separation occurs and 3D CFD models can be used to define geometry of heater tubes and dimensions to obtain uniform heat distribution load as well as refining The internal geometry of gas circuits where recirculation and stagnation occurs to minimize hydraulic resistance to the flow.

(Caetano et al., 2019) presented a methodology that aims not only to reduce the error in the prediction of the indicated power in beta-type Stirling engines below the 7% error found in models in literature, but also to facilitate extrapolation without the necessity of experimental data,1st order Schmidt method (*Hirata: Schmidt theory for Stirling engines—Google Scholar*, n.d.) was used to get pressure inside the engine exactly when the power piston is on the bottom dead center with an average error of 21.3%. CFD model at steady state (without piston movement) was used to get the temperature on displacer piston faces. In this methodology, the pressure and the temperature profile are respectively used as initial and boundary conditions for transient simulation. Also, the inclusion of the Discrete Ordinates radiation model increases the displacer's frontal face temperature by 132.2 K and results in an indicated power prediction improvement with an error reduction from −14.4% to −2.6% when compared to experimental values.

(Aboelsoud et al., 2014) studied the transport phenomena in a V-type corrugated carbon foam, investigating foam with various lengths and heights the study concluded that there is a length at which heat transfer efficiency of the foam approaches unity and after this distance no significant heat transfer occurs this distance was found to be 3 times the pore size and this finding can be useful to get the maximum heat transfer efficiency and decreasing pressure drop in the decreased length.

(Hachem et al., 2018) used CFD to study transport phenomena of Beta Stirling engine, the effect of porosity on convective heat transfer in regenerator deduced and comparison between 3 regenerator materials (copper, aluminum and stainless steel) was conducted concluding that copper is the best of them to be used in the regenerator.

C.Pan et al. used CFD to study heat transfer for oscillating flow in both helically coiled tube (Pan et al., 2014) and helically rectangular channel (Pan et al., 2018) heat exchanger.

It was observed in the literature that few researchers studied the shape of the regenerator. As stated by (Mahkamov, 2006) that 1st and 2nd order models are having a disadvantage that it represents the engine as one-dimensional, this problem can be solved by using CFD models in which dealing with different geometries taking into account their effects the different parameters are possible. In this work, a simple CFD model for simulating an alpha type Stirling engine was developed. Results were validated against the work of (Almajri et al., 2017) based on indicated power. The study is then extended, changing the geometry of the regenerator and using a V-type regenerator in the light of the work of (Aboelsoud et al., 2014) the effect of regenerator geometry on indicated work is being realized.

2. CFD MODEL:

A CFD model is developed using COMSOL Multiphysics (*COMSOL Multiphysics, '"5.0 a, COMSOL Inc."'.*, n.d.) to characterize transport mass and heat in the regenerator of an alpha-type Stirling engine. The geometry was created as a 2D CAD model using SolidWorks, as shown in Figure 1. Parameters of the engine to be modeled are listed in Table 1. Figure 1 shows the geometry of the engine, the differential equations used to solve for the transport phenomena are the continuity equation, Navier-Stokes and Brinkman equations, and the energy equation. Moving mesh was employed to account for the changes in the geometry of the domain due to the movement of the pistons. The materials used are as follows, pistons are solid made of Steel, the solid part of the regenerator located at the center of the geometry is made of Nickel chrome with 110 μm wire diameter, and the working gas is air treated as an ideal gas.

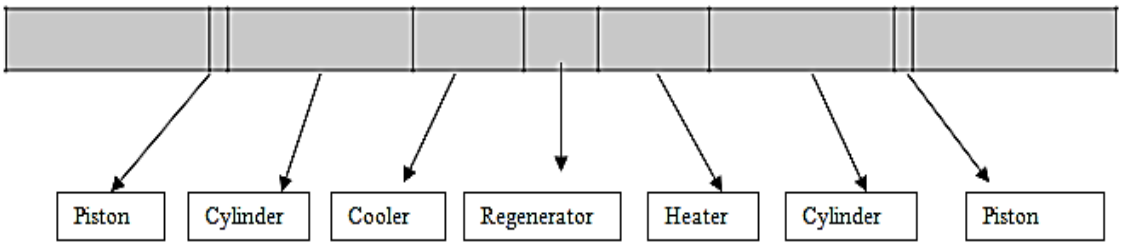

Figure 1: Engine geometry

2.1. Governing equations:

Comsol Multiphysics is used to solve the differential equations describing the different transport phenomena occurring in the different domains. Firstly a moving mesh was chosen with prescribed deformation to account for the changing volumes in the geometry due to pistons movement. The two pistons move with an optimum phase shift of 90 degrees between them based on different studies found in the literature. The equations for the movement of the pistons are as follows:

$$Xp1 = a0\,(\cos(\theta)) \quad (1)$$

$$Xp2 = a0\,(\cos(\theta + \alpha)) \quad (2)$$

$$\theta = \frac{2\,(\pi)(N)(t)}{60} \quad (3)$$

Table 1: Parameters of the engine

Parameter	Value	Parameter	Value
Th	**1373 K**	**Vregenerator**	**2.01X10^-5 m^3**
Tc	**293 K**	**Pcharge**	**2 Bar**
Vsc	**0.000134303 m^3**	**Tcharge**	**293**
Vse	**0.000134303 m^3**	**α**	**90**
Vclc	**3.534X10^-6 m^3**	**Θ**	**Crank angle**
Vcle	**3.534X10^-6 m^3**	**N**	**555 RPM**
Vcooler	**4.24X10^-5 m^3**	**Ɛp**	**0.711**
Vheater	**4.24X10^-5 m^3**		

Figure 2 shows the volume variation in both the compression and expansion spaces over the engine cycle with respect to the crank angle, and the two curves resemble the volume variations of the engine spaces for the engine studied by Almajri (Almajri et al., 2017).

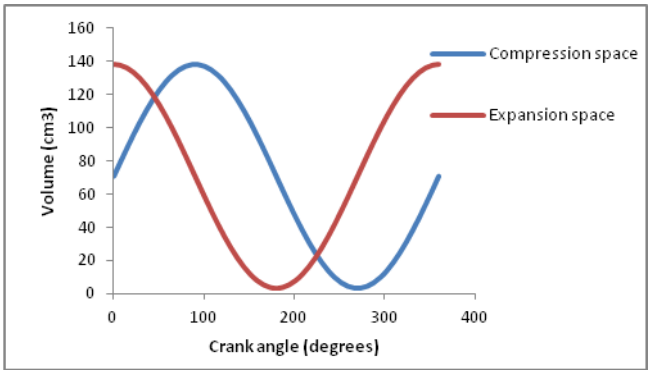

Figure 2: Variation of compression and expansion spaces within an engine cycle for N=555 r.p.m

Secondly, fluid was modeled using free and porous media flow physics with equations describing flow of the working fluid in both the porous media and the free media.
Equations are as follows:

Continuity equation or mass conservation equation

$$\frac{\partial \rho}{\partial t} + \nabla.(\rho u) = 0 \quad (4)$$

Where the 1st term represents the change in mass in control volume and the 2nd term represents the change in mass at the control surface.

Momentum conservation equation

$$\rho \frac{\partial u}{\partial t} + \rho(u.\nabla)u = \nabla.\left[-PI + \mu(\nabla u + (\nabla u)^T) - \frac{2}{3}\mu(\nabla.u)I\right] + F \quad (5)$$

Where the local and convective derivatives in LHS represent inertial forces and the 1st term in the right-hand side represents the pressure forces, the 2nd and 3rd term represent viscous forces, and the 4th term represents any volume force source term, and in this work, this last term is equal to zero(Munson, 2010,Fundamentals of fluid mechanics, Wiley).
For the porous media same equations imply but with some modifications to account for porosity effects

$$\frac{\partial(\varepsilon_p \rho)}{\partial t} + \nabla.(\rho u) = Q_{br} \quad (6)$$

Where Q_{br} is any mass source term and is equal to zero.

$$\frac{\rho}{\varepsilon_p}\left(\frac{\partial u}{\partial t} + (u.\nabla)\frac{u}{\varepsilon_p}\right) = \nabla.\left[-PI + \frac{\mu}{\varepsilon_p(\nabla u + ([\nabla u])^T)} - \frac{2\mu}{3\varepsilon_p}(\nabla.u)I\right] - \left(\mu k^{-1} + \beta_F|u| + \frac{Q_{br}}{\varepsilon_p^2}\right)u + F \quad (7)$$

The permeability of porous material can be calculated using the hydraulic diameter, which can be found using wire diameter from the following equation:

$$d_h = \frac{\varepsilon_p}{1-\varepsilon_p} d_w \quad (8)$$

$$k = \frac{2 d_h^2}{a_1} \quad (9)$$

Where (a1) is a constant taken as 123.

Forcheimer drag can be calculated from the following equation

$$\beta_F = \frac{C_F \rho}{\sqrt{k}} \quad (10)$$

$$C_F = \frac{3.5}{\sqrt{150.\varepsilon_p^2}} \quad (11)$$

Finally, Heat transfer in porous media physics was added with heat transfer in fluids and heat transfer in solids added. They were fully coupled with flow physics to account for heat transfer in fluid domains, solid domains, and regenerator (porous) domain. The governing equation is the energy conservation equation.

$$d_z \rho C_p \frac{\partial T}{\partial t} + d_z \rho C_p u.\nabla T = \nabla.(d_z K \nabla T) + d_z Q + Q_{vd} + Q_p + Q_{ocp} \quad (12)$$

It must be noted that working fluid is treated as ideal gas so:

$$\rho = \frac{P_A}{R_S T} \quad (13)$$

For solid domains (the two pistons):

$$d_z \rho C_p \frac{\partial T}{\partial t} + d_z \rho C_p u . \nabla T = \nabla . (d_z K \nabla T) + d_z Q + Q_{oop} \quad (14)$$

For porous media

$$d_z (\rho C_p)_{eff} \frac{\partial T}{\partial t} + d_z \rho C_p u . \nabla T = \nabla . (d_z K_{eff} \nabla T) + d_z Q + Q_{vd} + Q_p + Q_{oop} \quad (15)$$

The work done by pressure changes (Q_p) and the viscous dissipation in fluid (Q_{vd}) are negligible.

$$[(C)_p]_{eff} = \theta_p \rho_p C_{p,p} + (1 - \theta_p) \rho C_{\square} \quad (16)$$

$$K_{eff} = \theta_p K_p + (1 - \theta_p) K \quad (17)$$

$$\theta_p = 1 - \varepsilon_p \quad (18)$$

2.2. Boundary and Initial conditions:

For solving differential equations some boundary and initial conditions must be defined, for fluid flow physics two initial conditions are defined these are pressures above and below the pistons where the pressure above the piston is the charge pressure whereas below the piston is atmospheric pressure. The unsteady time dependant solution of the governing equations was initialized by a stationary solution for heat transfer only and without any piston movement. Pressures and temperatures from the steady-state solution were taken as initial conditions for the fluid and heat transfer equations, respectively. The boundary conditions defined are moving walls at pistons to account for their motion with their velocities taken from moving mesh, slip walls at the cylinders and the regenerator and no-slip walls at the cooling and heater walls, an outlet boundary condition was defined at the back of the pistons where pressure was defined as atmospheric to neglect compression occurring at the back of the pistons. Figure 3 shows the different boundary conditions for fluid flow. For heat transfer, the boundary conditions defined are insulated walls in addition to prescribed temperatures at the heater and cooler walls to account for the two heat exchangers. Figure 4shows Boundary conditions for heat transfer.

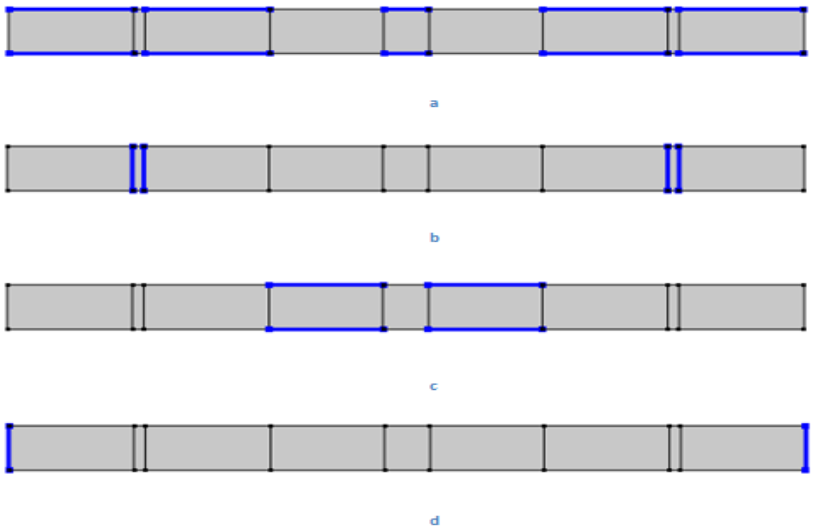

Figure 3: a-slip b-moving walls c-no-slip d-outlet

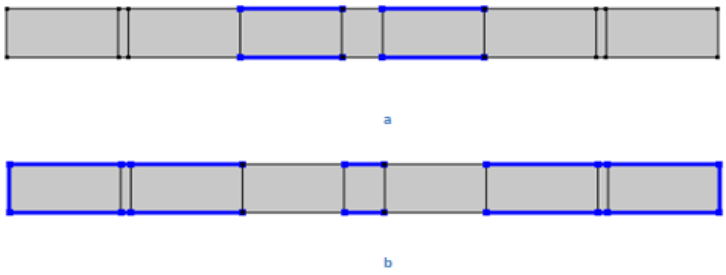

Figure 4: a-Temperature boundary condition b-insulated walls

3. MODEL VALIDATION:

The 2d CFD model was validated against the work of Al-Majri [6] based on pressures, volumes, and total indicated power. As shown in Figure 2 that the two engines have similar volume variation. Figure 5and Figure 6 show P-V diagrams for expansion and compression areas for both models. The maximum pressures decrease in the current model. This can be attributed to some differences in the clearance volume between the two models in addition to the small difference in charging temperature. The indicated power was 146 W for the model developed by AlMajri [6] while it was 125W for this work. The error ranges from 6.5% to a maximum error of 18%.

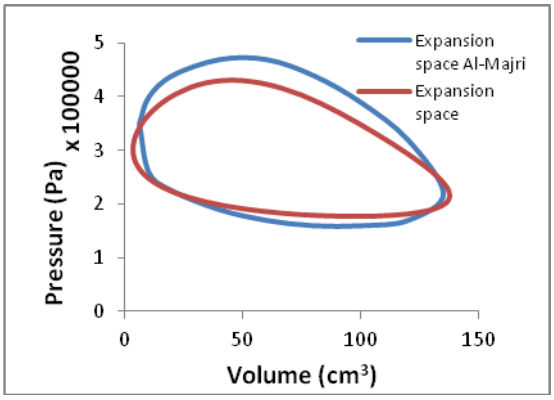

Figure 5: P-V diagrams for expansion area for Thermodynamic and CFD models

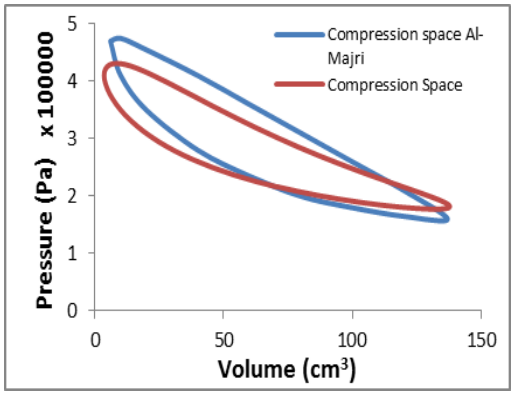

Figure 6: P-V diagrams for compression area for (Almajri et al., 2017) vs. Current work

3.1. Mesh Independence:

The mesh used for this study had a grid density of (61102) elements and an average quality of (0.9385), mesh independence test was performed for coarse, Normal, fine and extremely fine meshes with different number of elements. Figure 7 shows the result of the test, the difference between results from coarse and finer mesh was 30% and between the finer and extremely fine was 4%. Free triangular, quadrilateral meshes were used; boundary meshing and corner refinements were done.

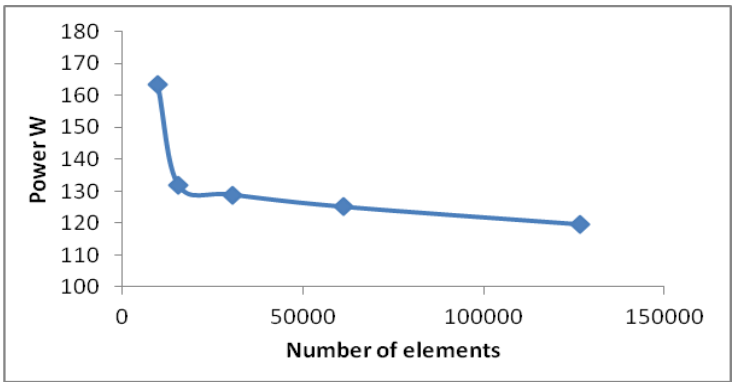

Figure 7: Mesh Independence test

4. NOVEL GEOMETRY:

W.Aboelsoud (Aboelsoud et al., 2014) studied the flow and heat transfer through V-type corrugated carbon foam for different dimensions, using the developed CFD model the effect of changing regenerator geometry to a V-type corrugated geometry in oscillating flow on the indicated power was investigated. Figure 8 shows the novel geometry of the regenerator, the length of the V-type corrugated geometry was chosen to be 30mm,the width was 38.1 mm, and the V-angle was 3.76 degrees.

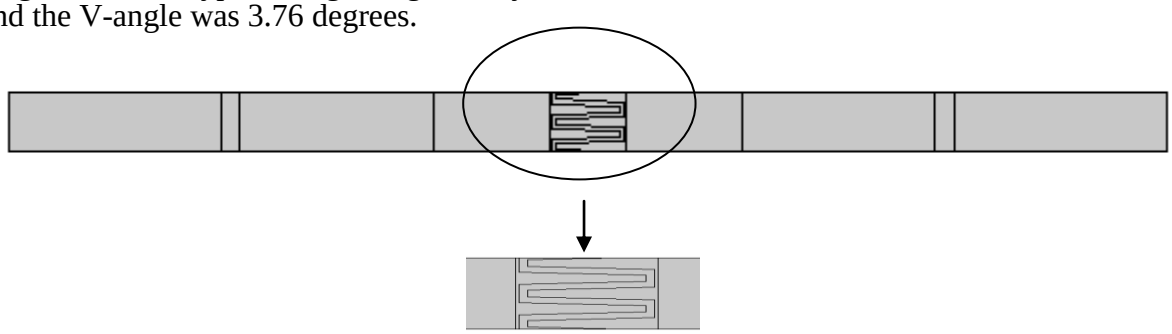

Figure 8 Novel geometry

5. RESULTS AND DISCUSSION:

During the study, different charging pressures were investigated (1.5, 2, 2.5 Bars) the relation between charging pressure and indicated work output is shown in Figure 9. It can be concluded that as charging pressure increases, indicated work increases. This result agrees with the results obtained by Almajri (Almajri et al., 2017). Figure 10 shows the effect of changing the temperature at heater walls on engine indicated power at the same cooler temperature. It can be concluded that as heater temperature increases indicated power of engine increases. Figure 11 shows the P-V diagram for the engine after changing its regenerator's geometry, the P-V diagram of the compression space nearly coincides with the expansion space. Table 2 shows the dimensionless work for novel geometry at different conditions. The dimensionless work is defined as:

$$Wdimensionless = \frac{W}{mRTe} \qquad 19$$

The dimensionless work of the novel geometry was 0.011 compared to 0.065 for the original regenerator geometry this decrease in work can attributed for a higher temperature at compression space and lower temperature at expansion space, this decrease in heat transfer between regenerator and working fluid was also accompanied by a decrease in the pressure drop which can be attributed low area ratio between the novel geometry and the original regenerator and also for the high speed of the engine, decreasing the speed resulted in dimensionless work of 0.018 and an increased average temperature at expansion space it must be noted that the power output decreases as the time required to complete one cycle increases,

increasing the wall thickness resulted in a further decrease in dimensionless work as an increase in temperature of the expansion space was observed, increasing the apex angle resulted in a small increase in dimensionless work as a decrease in the temperature of both compression and expansion spaces was observed. One of the observations of the 2-D model is that the pressure drop across the regenerator was negligible and was in the order of 100 Pa; this result was less than expected and may need further study by developing a 3-D model.

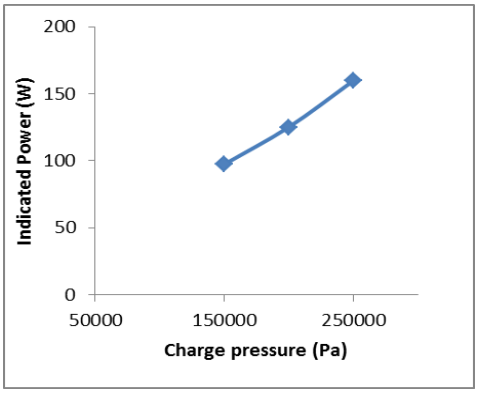

Figure 9 Effect of Charge Pressure

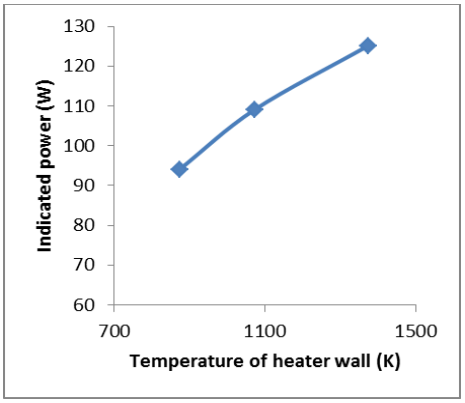

Figure 10 Effect of Temperature at Heater Walls

Table 2: Dimensionless work for novel geometry at different conditions

No.		angle	Thickness	RPM	Te	Tcomp	$W_{dimensionless}$	Area	Area ratio
1	Original geometry			555	1242	398.6	0.065021	1200	
2	Novel geometry	3.76	2.5	555	1142	608	0.011298	439.9	36.65833
3	Novel geometry	3.76	2.5	50	1240	467	0.018581	439.9	36.65833
4	Novel geometry	3.76	6	555	1212	633	0.010693	750	62.5
5	Novel geometry	5	2.5	555	1106	541	0.011458	441.6	36.8

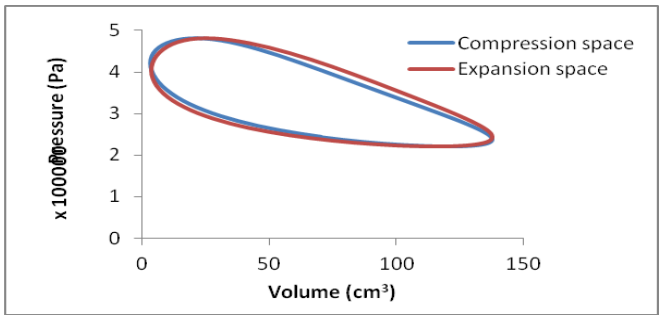

Figure 11 P-V diagram for the engine with a novel geometry

6. CONCLUSION

A 2-D CFD model was developed for an alpha type Stirling engine and validated against the model developed by Al-Majri (Almajri et al., 2017), results showed good agreement of the indicated power and P-V diagrams between both models. The validated model was used to investigate the effect of some parameters on indicated power and the effect of changing regenerator volume to a V-type corrugated porous media. The performance of the engine with the novel geometry was investigated using a dimensionless work parameter. For the novel

geometry, it was found that the dimensionless power was lower than that of the original geometry, the work was decreased because of a decreased heat transfer between the working fluid and the regenerator through the channels at this high engine speed, effects of changing the apex angle, the thickness of porous media and the engine speed on the engine performance were investigated it was found that the engine performance was improved when the engine worked at lower speed, the dimensionless work parameter increased when the apex angle was increased to 5 degrees while it decreased when the wall thickness increased. One of the observations of the 2-D CFD model was that the pressure drop across the regenerator was less than expected. It is expected to extend the study to a 3-D model for better visualization of flow and pressure drop across regenerator in addition to validation of the obtained results through experimental work in future work.

REFERENCES:

1. Aboelsoud, W., Wu, W., Chow, L. C., Saarloos, B. A., & Rini, D. P. (2014). Analysis of thermal and hydraulic performance of V-shape corrugated carbon foam. International Journal of Heat and Mass Transfer, 78, 1114–1125. https://doi.org/10.1016/j.ijheatmasstransfer.2014.07.042
2. Ahmed, H., Almajri, A. K., Mahmoud, S., Al-Dadah, R., & Ahmad, A. (2017). CFD modelling and parametric study of small scale Alpha type Stirling Cryocooler. Energy Procedia, 142, 1668–1673. https://doi.org/10.1016/j.egypro.2017.12.547
3. Alexakis, T. (2013). CFD modelling of Stirling engines with complex design topologies [Doctoral, Northumbria University]. http://nrl.northumbria.ac.uk/26308/
4. Alfarawi, S., AL-Dadah, R., & Mahmoud, S. (2016). Influence of phase angle and dead volume on gamma-type Stirling engine power using CFD simulation. Energy Conversion and Management, 124, 130–140. https://doi.org/10.1016/j.enconman.2016.07.016
5. Almajri, A. K., Mahmoud, S., & Al-Dadah, R. (2017). Modelling and parametric study of an efficient Alpha type Stirling engine performance based on 3D CFD analysis. Energy Conversion and Management, 145, 93–106. https://doi.org/10.1016/j.enconman.2017.04.073
6. Caetano, B. C., Lara, I. F., Borges, M. U., Sandoval, O. R., & Valle, R. M. (2019). A novel methodology on beta-type Stirling engine simulation using CFD. Energy Conversion and Management, 184, 510–520. https://doi.org/10.1016/j.enconman.2019.01.075
7. COMSOL Multiphysics, '"5.0 a, COMSOL Inc."'. (n.d.).
8. Costa, S. C., Barrutia, H., Esnaola, J. A., & Tutar, M. (2013). Numerical study of the pressure drop phenomena in wound woven wire matrix of a Stirling regenerator. Energy Conversion and Management, 67, 57–65. https://doi.org/10.1016/j.enconman.2012.10.014
9. Costa, S. C., Barrutia, H., Esnaola, J. A., & Tutar, M. (2014). Numerical study of the heat transfer in wound woven wire matrix of a Stirling regenerator. Energy Conversion and Management, 79, 255–264. https://doi.org/10.1016/j.enconman.2013.11.055
10. Costa, S.-C., Tutar, M., Barreno, I., Esnaola, J.-A., Barrutia, H., García, D., González, M.-A., & Prieto, J.-I. (2014). Experimental and numerical flow investigation of Stirling engine regenerator. Energy, 72, 800–812. https://doi.org/10.1016/j.energy.2014.06.002
11. Hachem, H., Gheith, R., Aloui, F., Nasrallah, S. B., & Wang, M. (2018). A CFD Analysis of the Air Flow Through the Stirling Engine's Singularities. In F. Aloui & I. Dincer (Eds.), Exergy for A Better Environment and Improved Sustainability 1: Fundamentals (pp. 271–287). Springer International Publishing. https://doi.org/10.1007/978-3-319-62572-0_19
12. Hirata: Schmidt theory for Stirling engines—Google Scholar. (n.d.). Retrieved 15 February 2020, rom https://scholar.google.com/scholar_lookup?title=Schmidt%20theory%20for%20Stirling%20engines&author=K.%20Hirata&publication_year=1997
13. Mahkamov, K. (2006). Design Improvements to a Biomass Stirling Engine Using Mathematical Analysis and 3D CFD Modeling. Journal of Energy Resources Technology, 128(3), 203–215. https://doi.org/10.1115/1.2213273
14. Munson, B. R., Young, D. F., Okiishi, T. H., & Huebsch, W. W. (2010). Fundamentals of Fluid Mechanics: Student Value Edition (6th Edition Student Value edition). Wiley.

15. Pan, C., Zhang, T., Wang, J., & Zhou, Y. (2018). CFD study of heat transfer and pressure drop for oscillating flow in helical rectangular channel heat exchanger. International Journal of Thermal Sciences, 129, 106–114. https://doi.org/10.1016/j.ijthermalsci.2018.02.035
16. Pan, C., Zhou, Y., & Wang, J. (2014). CFD study of heat transfer for oscillating flow in helically coiled tube heat-exchanger. Computers & Chemical Engineering, 69, 59–65. https://doi.org/10.1016/j.compchemeng.2014.07.001
17. Tanaka, M., Yamashita, I., & Chisaka, F. (1990). Flow and Heat Transfer Characteristics of the Stirling Engine Regenerator in an Oscillating Flow. JSME International Journal. Ser. 2, Fluids Engineering, Heat Transfer, Power, Combustion, Thermophysical Properties, 33(2), 283–289. https://doi.org/10.1299/jsmeb1988.33.2_283